View Article Online / Journal Homepage / Table of Contents for this issue

New coordination polymer networks based on copper(II) hexafluoroacetylacetonate and pyridine containing building blocks: synthesis and structural study†

Silke Winter,[a] Edwin Weber,*[a] Lars Eriksson[b] and Ingeborg Csöregh*[b]

Received (in Montpellier, France) 29th March 2006, Accepted 8th September 2006
First published as an Advance Article on the web 9th October 2006
DOI: 10.1039/b604591j

Published on 09 October 2006 on http://pubs.rsc.org | doi:10.1039/B604591J
Downloaded by University of California - Los Angeles on 01 January 2013

The interaction between copper(II) hexafluoroacetylacetonate [Cu(hfacac)$_2$] and pyridine-containing building blocks with linear, angled and trigonal geometry (**1–3**) has led to isolation of different coordination polymers (**A–D**). These were studied by infrared spectroscopy and single-crystal X-ray diffraction methods. The copper coordination geometry in the present complexes can be described as a more or less distorted square bipyramid (or elongated octahedron). The unsaturated Cu(hfacac)$_2$ units are connected by the aromatic spacer ligand moieties **1–3** so as to form polymeric frameworks, which are infinite either in one (**A** and **D**) or in two dimensions (**C**). The polymeric ropes or sheets are held together in the crystals by relatively weak intermolecular interactions, in which the protruding fluoro substituents of the metallic links play an active role. The porous compound **A** was also studied with respect to sensing reactions for potential analysis of selected volatile compounds. The screening shows interesting reactions of this coordination polymer, indicating a reversible response of relatively small and polar analytes such as methanol, ethanol and acetone, but not of water.

Introduction

One of the most important current developments in chemical research involves the design and study of organic–inorganic hybrid materials of coordination polymer type, composed of metal ions and multifunctional organic ligands.[1] In particular, they may feature open frameworks, thus being zeolite-like but having intrinsic advantages over conventional porous materials because of structural variety.[2] The strong interest in this field is due to the promising applications in size- or shape-selective catalysis, molecular electronics, optics, chemical sensing and fuel storage.[3] In this connection, some control over the topology and type of the supramolecular coordination network can be achieved by suitable choice of organic ligand,[1] metal coordination preference,[4] inorganic counter ion,[5] solvent[6] and ligand-to-metal ratio.[7] Nevertheless, the organic ligand with its properties such as coordination activity, solubility, geometry, length and orientation of the donor sites has one of the key functions in designing defined network structures. Here, aside from carboxylate and imine functions, bridged bidentate pyridyl and nitrile ligands are perhaps the most commonly used donor groups in coordination polymers.[1,8]

However, a great problem connected with the design of polymeric coordination compounds is the formation of a penetrated network architecture having very low porosity.[9] Moreover, channels that are initially filled with solvent molecules usually lose their stability if the guest molecules are removed.[10] In order to meet these problems, a combination of the principles usually applicable to coordination polymers,[1] on the one hand, and those of dominantly organic crystal engineering,[11] on the other, has been used to evolve a promising new approach.[12] The aim is to get control of the properties of a crystalline material *via* adaptation of the whole crystal topology. Therefore, aside from the metal coordination parameters, a profound understanding of the wide diversity of noncovalent interactions in solid state materials, typical of crystal engineering, is required.[13,14]

Considering this approach, in an unsaturated metal complex containing a fluorinated organic ligand, the tendency of the organic fluorine to be engaged in hydrogen bonding and F···F interactions is expected to be rather low, although the background of these facts is currently very controversial and subject to discussion.[15] Nevertheless, organic fluorine can play a significant role in the design of solid materials,[16] just because of its repulsive behaviour preventing potential penetration of a network.[17] Also, an electron-withdrawing fluoro substituent on the organic ligand will alter the complex stability, which may be a supporting effect in the formation of the coordination network, relating to the 'directional bonding principle'[18] discussed in more detail later in this paper (synthesis of the

[a] *Institut für Organische Chemie, TU Bergakademie Freiberg, Leipziger Str. 29, D-09596 Freiberg/Sachsen, Germany. E-mail: edwin.weber@chemie.tu-freiberg.de; Fax: +49 3731-39-31 70*
[b] *Department of Structural Chemistry, Arrhenius Laboratory, Stockholm University, S-10691 Stockholm, Sweden. E-mail: ics@struc.su.se; Fax: +46 8 163118*

† Electronic supplementary information (ESI) available: Non-covalent interactions in complex **A** (Table S1), geometric details of the tris(pyridylethynyl)benzene ligand moieties in complexes **C** and **D** (Table S2), non-covalent host–guest interactions in complex **D** (Table S3), and non-covalent inter-chain connections in complex **D** (Table S4). See DOI: 10.1039/b604591j

 This journal is © the Royal Society of Chemistry and the Centre National de la Recherche Scientifique 2006

Downloaded by University of California - Los Angeles on 01 January 2013
Published on 09 October 2006 on http://pubs.rsc.org | doi:10.1039/B604591J

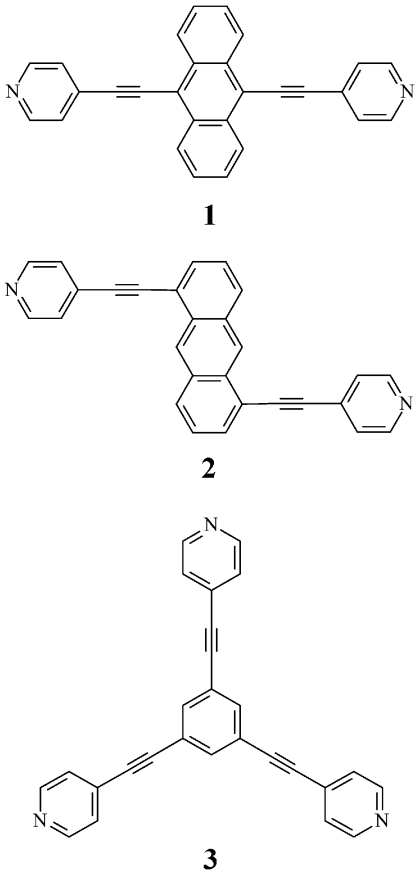

Scheme 1 Tectonic coordinative spacer units **1–3**.

coordination polymers). Hence, a modular construction set for assembly of desirable polymeric coordination frameworks has been developed, comprising oligofunctional tectons of monodentate pyridyl type as coordinative spacer units (Scheme 1) and coordinatively unsaturated copper(II) hexafluoroacetylacetonate [Cu(hfacac)$_2$] as the connecting metallic link essential to the approach (Scheme 2).

The synthesis and characterization of the respective compounds, as well as crystal structures representative of the new coordination polymers, are described; and properties of reversible vapour sorption/desorption involving the new materials are reported.

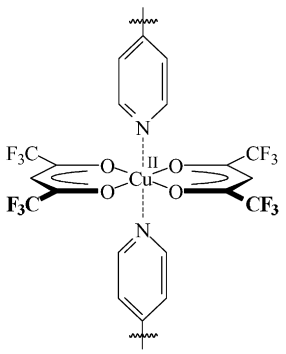

Scheme 2 Desired configuration of the coordination environment of the copper(II) ion. Only the active sites of the tectonic ligands in the coordination sphere are shown.

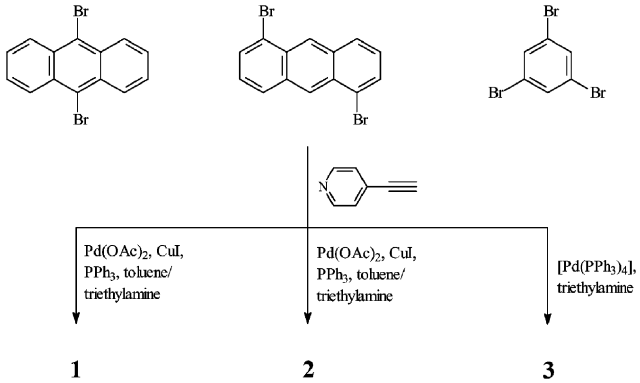

Scheme 3 Synthesis of the tectonic units **1–3**.

Results and discussion

Synthesis of the tectonic ligands

Syntheses of the ligands **1**, **2** and **3** (Scheme 1) were performed, using the method of Sonogashira[19] as the key reaction step. In this process a coupling reaction between a terminal alkyne and a halogenated aromatic compound is effected. As applied to the present task, cross-coupling reactions of 4-ethynylpyridine with the corresponding aryl bromides were carried out to yield the tectonic ligands **1–3**, following described procedures for **1**[20] and **3**[21] (although the catalytic systems used were different, and the characterization of the compounds is somewhat incomplete), whereas ligand **2** is a completely new compound (Scheme 3). The key component 4-ethynylpyridine was prepared by palladium(0) coupling of 4-bromopyridine hydrochloride with 2-methyl-3-butyn-2-ol (MEBYNOL)[22] followed by abstraction of the protecting group with NaOH in toluene, according to the literature.[22]

Synthesis of the coordination polymers

The principal procedure used for the formation of the present coordination polymers corresponds to the so-called 'directional bonding approach' which is a strategy adopted for the construction of supramolecular compounds through coordination chemistry.[23] It means that, in the first instance, a coordinatively unsaturated metal complex is required in directing the other ligands intended for coordination to the appropriate place of the coordination sphere of the metal ion. Hence, copper(II) hexafluoroacetylacetonate was selected as the coordinatively unsaturated complex (Scheme 2). Here, the metal centre is poorer in electrons than in normal copper (II) acetylacetonate. According to a suggestion of Stang,[23] "rigid highly directional multibranched monodentate ligands, which bind to partially coordinatively unsaturated transition metal complexes *via* dative bond interaction" should be used, such as the tectons **1**, **2** and **3** (Scheme 1). They are intended to form bridges between the metal centres in order to create the polymeric compounds. Here, it should be remarked that compound **3** has proved to be very useful for the self-assembly of discrete (*i.e.* nonpolymeric) polyhedral structures and nanosized supramolecular cages.[24]

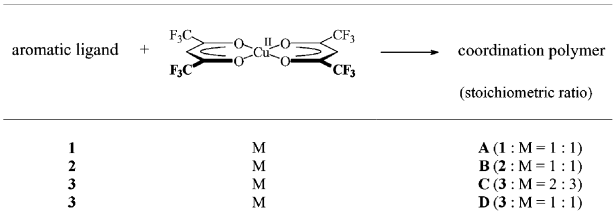

Scheme 4 Coordination polymers (**A–D**) formed of **1–3** with copper(II) hexafluoroacetylacetonate (M).

Published on 09 October 2006 on http://pubs.rsc.org | doi:10.1039/B604591J
Downloaded by University of California - Los Angeles on 01 January 2013

For the synthesis of the different coordination polymers, separate solutions of the two components, tectonic ligand and copper(II) hexafluoroacetylacetonate, in chloroform were prepared and combined by addition of the metal-complex solution to the solution of the ligand in a stoichiometric amount. In the case of the coordination polymers **A** and **B**, a ratio (L : M) of 1 : 1 was used, and for **C** a ratio of 2 : 3 (Scheme 4). The polymers **A**, **B** and **C** were obtained as microcrystalline solids, which were characterized by IR spectroscopy and elemental analysis.

Using ligand **3** and $Cu(hfacac)_2$ in a 1 : 1 ratio yielded solvated crystals of coordination polymer **D**, which are however unstable at room temperature when not immersed in the mother liquor, due to solvent evaporation.

IR spectroscopic characterization

The successful complexation of the tectonic ligands **1–3** to $Cu(hfacac)_2$ was checked by IR spectroscopy. IR spectra were collected of all compounds involved [ligands **1–3**, $Cu(hfacac)_2$ and the coordination polymers **A**, **B** and **C**] for comparison (Table 1). Obvious differences are shown by the bands that come from the $Cu(hfacac)_2$ unit. The valence vibration of the carbonyl group was assigned at 1647 cm^{-1} in $Cu(hfacac)_2$.[25] This band is shifted by nearly 20 cm^{-1} towards higher frequencies in the polymeric compounds, indicating stabilization of the bond by formation of the new environment of the complex unit. That is to say, the complexation of the pyridine-containing ligands reduces the electronegativity of the metal centre in the $Cu(hfacac)_2$ unit. Unfortunately, the bands in the region 1646–1599 cm^{-1} of the polymeric complexes could not be clearly identified because of superimposition of the aromatic (C=C) and the shifted (C=O) stretching frequencies of the complex unit. The same shift tendency can be observed for the (CH) deformation vibration of the chelate ring. Moreover, the valence vibration of the CF_3 group is rather specifically affected in the coordination polymers. While the band at 1229 cm^{-1} is shifted towards lower frequencies, the band at 1145 cm^{-1} remains fairly constant. The deformation vibration of the CF_3 groups at 791 cm^{-1} as well as the deformation of the chelate ring at 662 cm^{-1} are also shifted towards lower frequencies in comparison with $Cu(hfacac)_2$. However, the influence on the Cu–O bond attributed to the tectonic coordination could not be observed due to overlapping and low intensity of the bands. Besides, in coordination polymer **A**, the shift of the (C≡C) valence vibration at 2208 cm^{-1} in the free ligand **1**[20] to 2197 cm^{-1} in the polymeric complex is a remarkable finding, which is an indication of the changed molecular environment of the (C≡C) bond. By way of contrast, the spectrum of coordination polymer **B** does not show an analogous shift.

Crystal structures

The coordination polymers **A**, **C** and **D** (Scheme 4) have been investigated using X-ray diffraction on single crystals. Complex **D** proved to be a chloroform-containing solvate in a very unstable form, since the crystals rapidly decomposed into powder at room temperature when taken out of the solution. Nevertheless, we managed to collect X-ray intensity data at low temperature (183 K), and to solve the crystal structure of this compound. Crystals of complex **B** were also obtained, but their quality was not good enough for a single-crystal diffraction study.

Fig. 1–6 illustrate the investigated crystal structures. Crystal data and details of the X-ray data reduction and structure refinement calculations are listed in Table 2. Selected geometric features of the copper coordination polyhedra in **A**, **C** and **D** are presented in Table 3, and Tables S1–S4 (ESI†) show geometric features of ligand **3** in crystals **C** and **D**, as well as the most noteworthy non-covalent interactions and intermolecular contact distances in the different species.

The Cu(II) centre ions in the present three complexes (*i.e.* **A**, **C** and **D**) are all sixfold coordinated, each surrounded by four oxygen and two nitrogen atoms. The O ligand atoms are donated by two hexafluoroacetylacetonate (hfacac) groups, and the N atoms are coming from the adjacent pyridyl rings, which belong to the connecting (spacer) ligand moieties (Scheme 2). The copper coordination geometry can be described as a more or less distorted octahedron (or square bipyramid).[26] Two of the ligand oxygens and the two nitrogen

Table 1 Comparison between the IR data of $Cu(hfacac)_2$ and the complex unit in the coordination polymers **A**, **B** and **C**

Specification	$[Cu(hfacac)_2]$	Complex **A**	Complex **B**	Complex **C**
ν(C=O)	1647 (1615)	1671	1669	1671
ν(C=C) chelate ring + ν(C=O)	1561 1535	1646–1599	1646–1613	1647–1601
δ(CH) chelate ring	1484–1468	1532–1512	1532–1509	1532–1513
ν(C=C) chelate ring	1257	1256	1257	1257
$\nu(CF_3)$	1345			
	1229	1203	1210	1203
	1145	1151	1150	1148
$\delta(CF_3)$	807	791	794	792
δ(chelate ring)	676	662	662	662
$\delta_s(CF_3)$	594	577	577	578

 This journal is © the Royal Society of Chemistry and the Centre National de la Recherche Scientifique 2006

Downloaded by University of California - Los Angeles on 01 January 2013
Published on 09 October 2006 on http://pubs.rsc.org | doi:10.1039/B604591J

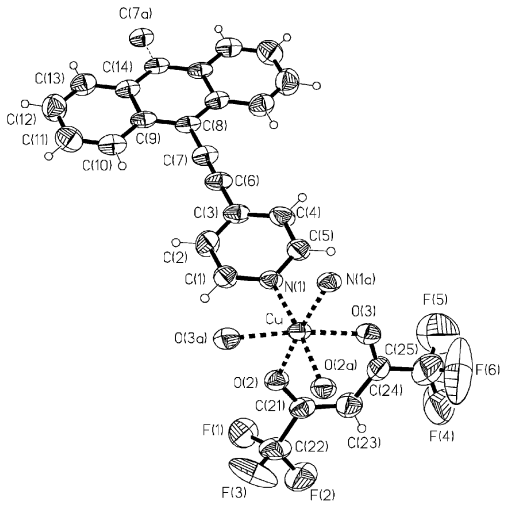

Fig. 1 Perspective view of a characteristic fragment of the polymeric **A** complex. The unique atom positions, and four adjacent symmetry-generated ones [N(1a), O(2a), O(3a) and C(7a)], are labelled. The atomic displacement ellipsoids of the non-hydrogen atoms are drawn at 30% probability level.

atoms, coordinated by nearly equal bond lengths of ~2 Å (Table 3), define the approximately square planar coordination plane, whereas the two remaining O ligand atoms, linked *via* the longer Cu–O distances (~2.2–2.3 Å), occupy the axial positions, nearly at right angles to the equatorial plane. The unsaturated $Cu(hfacac)_2$ units are linked together by the

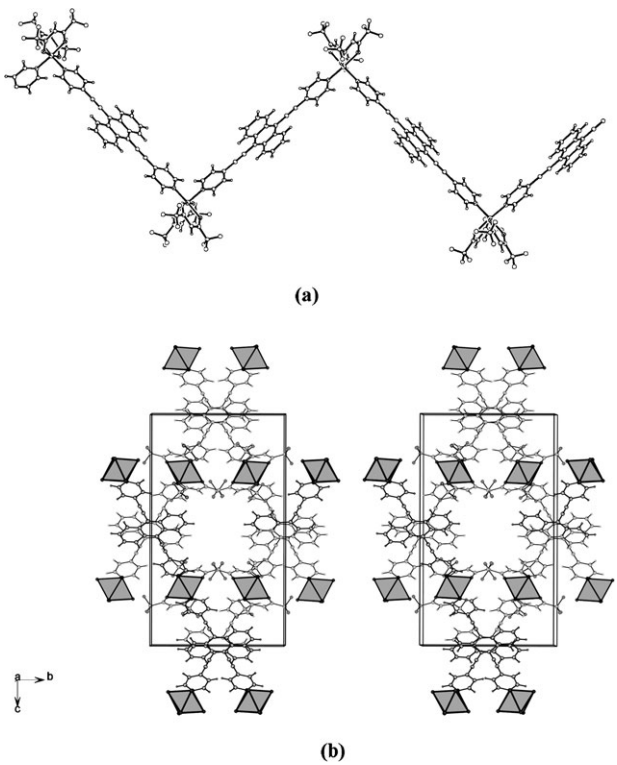

Fig. 2 Crystal packing of complex **A**. (a) Packing excerpt showing the infinite zigzag shaped polymeric chains. (b) Stereo packing illustration with the copper coordination indicated by shaded polyhedra.

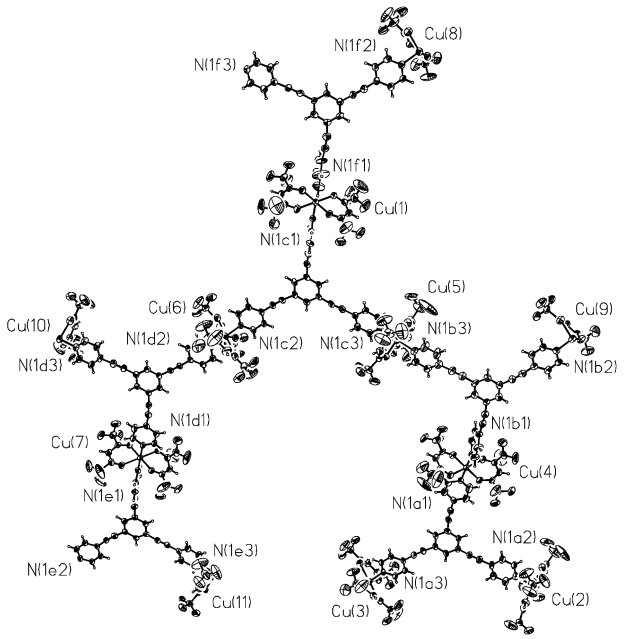

Fig. 3 Perspective view of the asymmetric unit of complex **C**. The atomic displacement ellipsoids of the non-hydrogen atoms are drawn at 30% probability level.

aromatic spacer ligand moieties **1–3** (Scheme 1) so as to form various polymeric frameworks, as specified below. The shortest Cu–Cu distances in the **A**, **C** and **D** crystals are 9.219(1), 7.856(2) and 8.544(2) Å, respectively.

(a) Coordination polymer A. In the orthorhombic crystal of complex **A**, both the metallic $Cu(hfacac)_2$ link and the tectonic spacer unit **1** exhibit crystallographic symmetry. As a consequence, the crystallographic asymmetric unit contains only one half of the $CuC_{10}H_2F_{12}O_4 \cdot C_{28}H_{16}N_2$ monomer (Fig. 1). The two pyridyl ring planes of the spacer (**1**) (both planar to within 0.009 Å) are centrosymmetrically related and co-planar, and both are only slightly tilted (8.7°) with respect to the anthracene plane within the same ligand moiety (the 14 anthracene C atoms are co-planar to within 0.035 Å).

The Cu^{2+} ion, located at the special position x, 1/4, 3/4, is exactly at the centre of the coordination polyhedron due to the crystal symmetry requirement, and out of the six coordinating ligand atoms only three (one N and two O) have unique (*i.e.* symmetry-independent) positions (Table 3). Moreover, the two coordinating hexafluoroacetylacetonate groups are also related by crystallographic symmetry due to the special location of the copper ion. Each hfacac moiety creates a six-membered chelate ring upon coordination to the metal ion (Scheme 2). The chelate rings are usually not entirely planar, although the O–C–C–C–O atoms of the acetylacetonate moiety are practically co-planar in most cases, in order to maintain the delocalization of the π-electrons. The Cu^{2+} ions, however, may deviate more or less from the plane formed by the five other ring atoms. This is the case in **A**, where the slightly puckered chelate ring was found to adopt an envelope conformation with the puckering parameters Q = 0.332 Å, θ = 124.6°, φ = 179.2°.[27–29] The best planes fitted to the two

Downloaded by University of California - Los Angeles on 01 January 2013
Published on 09 October 2006 on http://pubs.rsc.org | doi:10.1039/B604591J

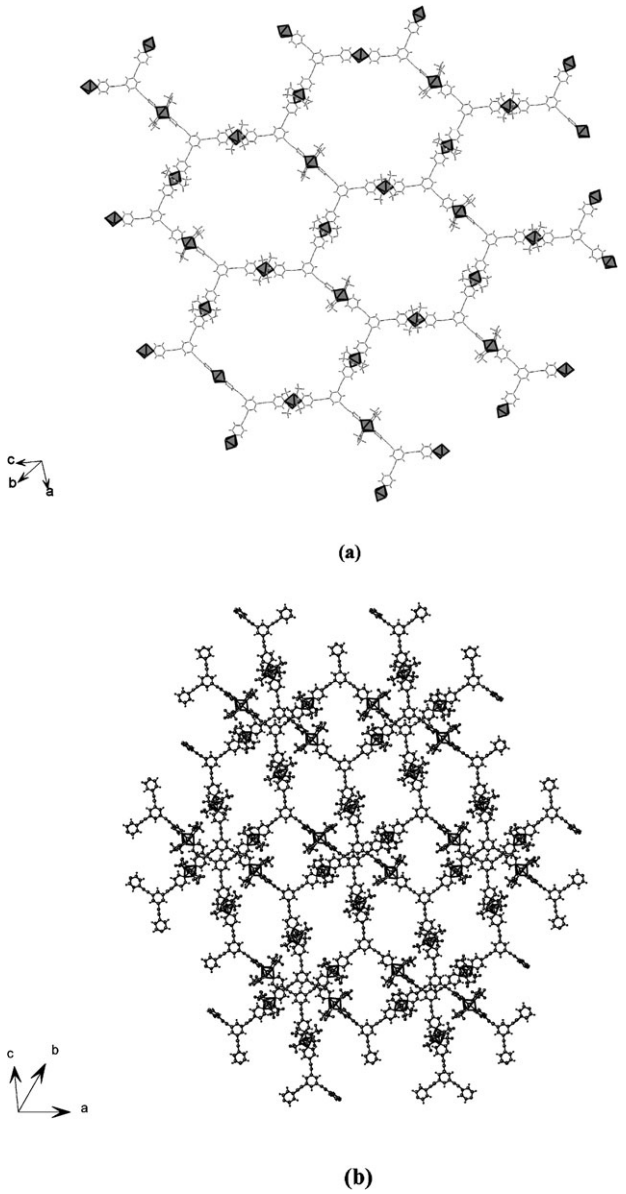

Fig. 4 Crystal packing of complex **C**. (a) Sheets showing infinite pattern of fused hexagons. The coordination is indicated by shaded polyhedra. (b) Packing illustration showing superposition of two consecutive polymeric sheets.

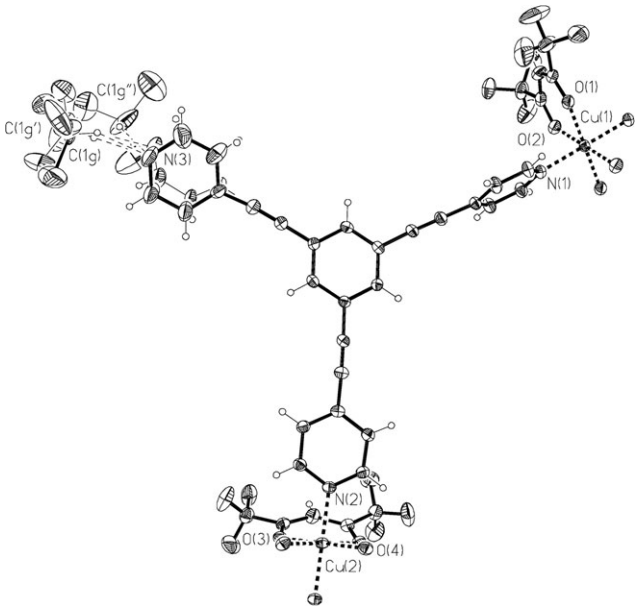

Fig. 5 Perspective view of the monomeric unit of the solvated complex **D**. The non-hydrogen atomic displacement ellipsoids are drawn at 30% probability level.

chelate rings with common copper centre form a dihedral angle of 65.7(1)°.

The N–Cu–N(#) coordination angle [where (#) means symmetry generated equivalent position] in the orthorhombic **A** crystal is 92.9(2)°, which gives rise to a '*cis*' orientation of the linear bidentate tectonic ligands containing N(1) and N(1#), respectively. As a consequence, the infinite polymeric chain progresses in zigzag fashion, taking a sharp turn with a nearly right angle at each metal ion centre [Fig. 2(a)].

Packing of the semi-rigid zigzag chains in the solid state leads to an arrangement with relatively low density (Table 2) and a low estimated value for the crystal packing index (56.2%).[29,30] The packing illustration [Fig. 2(b)] gives an indication of empty voids in the crystal, which could be confirmed by calculations.[29] Accordingly, in each unit cell a volume of 690 Å^3 (~16.6%) is accessible for possible solvent inclusion. Inspection of non-covalent connections (Table S1) shows that most of the shorter inter-chain distances are in the range of common van der Waals' contacts [$\sim(r_{vdW1} + r_{vdW2} + 0.2)$ Å; $r_{CvdW} = 1.70$, $r_{FvdW} = 1.47$, and $r_{HvdW} = 1.20$ Å],[29,31] thus suggesting relatively weak directional interaction forces in the observed F···F, C···F, (C–)H···O and (C–)H···F approaches[16,32] (Table S1).

Although the frequent occurrence of the fluoro substituents in shorter inter-chain connections may also be a consequence of the protruding position of the CF_3 groups (Fig. 2), it seems probable that the observed (C–)H···F connections are weak directional hydrogen bonds,[32,33] which in the absence of stronger interaction forces might affect the realized packing arrangement decisively.[34] Comparison with similar known interactions involving CF_3 groups supports this suggestion.[16] Worth noting is that according to our earlier experience,[35] the relatively low density and packing density may be an indication of the presence of directional intermolecular forces [such as (C–)H···O/F] in the crystal. However, the rigidity of the inconveniently shaped polymeric zigzag chains and the protruding stiff and bulky anthracene moieties may further enhance the difficulties of realizing a dense packing in crystal **A** [Fig. 2(b)]. A comparison with a recently published related crystal structure[20] seems to support this latter suggestion. Accordingly, infinite zigzag chains, similar to those of the polymeric **A** compound, have been observed in a Zn-containing complex, in which the four-fold coordinated Zn^{2+} ions are connected by bidentate 1,4-bis(4′-pyridylethenyl)tetrafluorobenzene spacer moieties.[20] Two linear aromatic ligands coordinate to each $Zn(NO_3)_2$ metallic link in a '*cis*' fashion, and the created zigzag chains realize a crystal packing arrangement which shows pronounced similarity to that of complex **A**.

 This journal is © the Royal Society of Chemistry and the Centre National de la Recherche Scientifique 2006

Published on 09 October 2006 on http://pubs.rsc.org | doi:10.1039/B604591J
Downloaded by University of California - Los Angeles on 01 January 2013

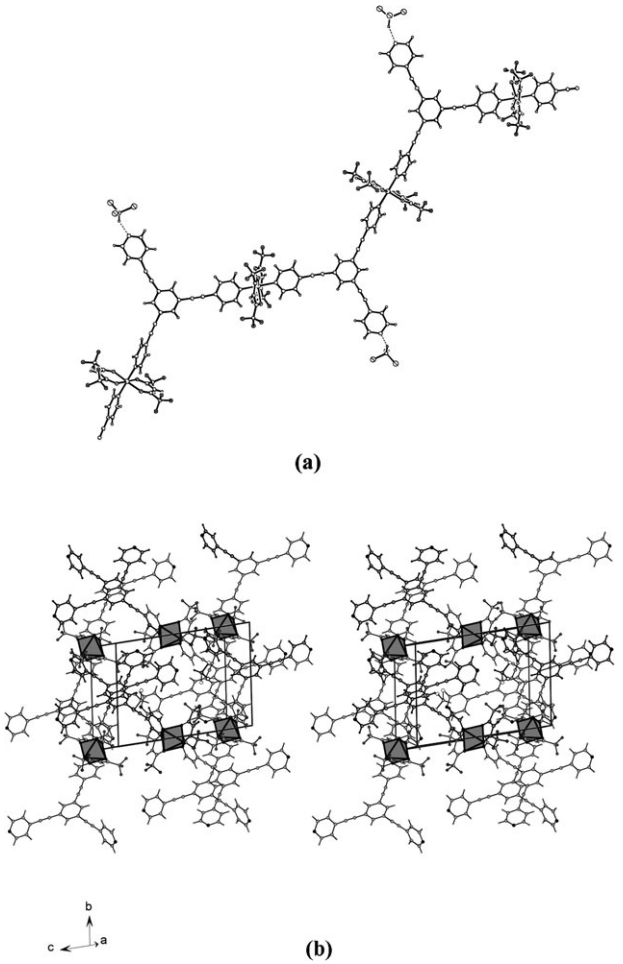

Fig. 6 Crystal packing of the solvated complex **D**. (a) Packing excerpt showing the infinite coordinatively polymerized chains possessing laterally attached solvent molecules of chloroform (minor disorder sites are omitted for clarity). (b) Stereo packing illustration with the coordination indicated by shaded polyhedra.

However, the Zn-containing crystal has somewhat lower symmetry (monoclinic $P2/c$) and significantly higher density ($D_{calc,X\text{-}ray}$ = 1.77 g cm^{-3}) than complex **A**. These differences may be attributed to the stiff protruding bulky anthracene moieties, which are present in the aromatic spacer links in complex **A**, but not in the Zn-containing one.

(b) Coordination polymer C. By analogy with structure **A**, when the Cu(hfacac)$_2$ units are linked together by the trifunctional three-pronged tectonic ligand **3**, such as in crystals of the **C** complex, the polymeric framework is expected to be infinite in two dimensions. In effect, diffraction studies of crystal **C** indicated endless polymeric sheets, similar to those observed earlier in a related complex compound with the three-connecting 2,4,6-tri(4-pyridyl)-1,3,5-triazine spacer units between the copper acetate dimers.[36] The crystal structures of these two green Cu-complexes exhibit pronounced similarities, but also notably differences. The methanol-solvated Cu-acetate complex[36] has monoclinic ($P2_1/n$) crystal symmetry with V_c = 3724.5(9) Å^3, whereas the crystallographic unit cell of complex **C** proved to have considerably larger volume [V_c = 13 795(6) Å^3] and lower crystal symmetry (triclinic P-1). Solution of the structure of compound **C** revealed that the crystallographic asymmetric unit is formed by nine Cu(hfacac)$_2$ complex entities and six tris(pyridylethynyl)benzene spacer moieties (Fig. 3). Seven unique copper centres [Cu(1)–Cu(7)] occupy general positions, whereas additional four Cu^{2+} ions [Cu(8)–Cu(11)] are located at special positions (each with 50% site occupation).

The copper coordination geometries can be described as more or less distorted square bipyramids also in complex **C** (Table 3). However, only four polyhedra [around Cu(8)–Cu(11)] exhibit crystallographic symmetry, whereas those connected to the Cu(1)–Cu(7) metal ions do not. Moreover, the N–Cu–N coordination angles also differ in **C** from the corresponding one in **A** (Table 3). Unlike the '*cis*' orientation of the bis(pyridylethynyl)anthracene ligands in **A**, all N–Cu–N coordination angles are nearly or exactly 180° (Table 3) in the triclinic **C** crystals, thus yielding a linear ('*trans*') orientation for the two pyridylethynyl groups at each copper centre [Fig. 3 and 4(a,b)]. The geometry of the different symmetry-independent Cu(hfacac)$_2$ complex units shows only modest variation (Table 3). The two chelate ring planes, which are joined by a Cu^{2+} ion in a special position, are co-planar (dihedral angle = 0.0°) due to the crystallographic symmetry, whereas those that are linked to a metal centre in a general position are more or less tilted with respect to each other, forming dihedral angles between 8.1(5) and 20.6(5)°. The average inter-chelate tilt angle, calculated for seven independent Cu(hfacac)$_2$ units without crystallographic symmetry, is 12.6[4.5]° (with the root mean square [rms] dispersion around the arithmetic average given in square brackets).

Comparison of the six unique tris(pyridylethynyl)benzene moieties (A–F) in complex **C** indicates important variations in their conformation. The three pyridyl rings in each tectonic ligand, which are supposed to have free rotation around the respective C≡C–C$_{py}$···N$_{py}$ axis, form significantly different dihedral angles with their central benzene ring plane in four moieties, namely in B, C, E and F (the tilt angles vary between 4.1 and 81.8°; Table S2†). Hence, these four ligands exhibit propeller-like shapes, which are however quite similar between themselves. By contrast, in two cases, namely in the A and D ligand entities (Fig. 3), the conformation is rather flat, since the pyridyl rings deviate only slightly from co-planarity with the benzene ring to which they are linked (the tilt angles vary between 4.9 and 9.1°; Table S2). In comparison, all tris(pyridyl)triazine spacer units in the Cu-acetate complex[36] exhibit the very same flat conformation.

In the crystal of **C**, the three-branched tris(pyridylethynyl)-benzene entities interlink the Cu(hfacac)$_2$ complex units so as to form infinite patterns of fused hexagons [Fig. 4(a)], just as in the polymeric sheets in the related Cu-acetate complex crystal.[36] The nice, apparently orderly, hexagonal arrangements have no crystallographic hexagonal symmetries, however. Deviation from the ideal symmetry is more pronounced in the case of the **C** complex, where the calculated distances between copper ions with diagonal locations in the hexagons vary between 32.3 and 37.8 Å [Cu(8)–Cu(9) = 32.37(1), Cu(3)–Cu(6) = 32.59(1), Cu(4)–Cu(7) = 34.700(6) and Cu(5)–Cu(11) = 37.77(1) Å; Fig. 3]. Moreover, orientation

View Article Online

Table 2 Summary of crystal data, experimental parameters and selected details of the refinement calculations for the complexes **A**, **C** and **D**

Compound	Complex **A**	Complex **C**	Complex **D**
Empirical formula (sum)[a]	$C_{19}H_9Cu_{0.5}F_6NO_2$	$C_{252}H_{108}Cu_9F_{108}N_{18}O_{36}$	$C_{38}H_{18}Cl_3CuF_{12}N_3O_4$
Empirical formula (moiety)[a]	$0.5[(CuC_{10}H_2F_{12}O_4)\cdot(C_{28}H_{16}N_2)]$	$9(CuC_{10}H_2F_{12}O_4)\cdot 6(C_{27}H_{15}N_3)$	$(CuC_{10}H_2F_{12}O_4)\cdot(C_{27}H_{15}N_3)\cdot(CHCl_3)$
Formula weight[a]	429.04	6587.42	978.44
Temperature/*K*	295(2)	293(2)	183(2)
Wavelength/Å	MoKα/0.710 73	MoK_α/0.710 73	CuKα/1.541 78
Crystal system	Orthorhombic	Triclinic	Triclinic
Space group (No.)	*Pnan* (No. 52)	$P\bar{1}$ (No. 2)	$P\bar{1}$ (No. 2)
a/Å	10.9340(10)	18.026(6)	9.9110(10)
b/Å	14.846(2)	29.133(5)	13.066(2)
c/Å	25.624(4)	30.927(8)	16.881(5)
α/°	90.0	63.44(2)	97.810(10)
β/°	90.0	78.13(3)	105.820(10)
γ/°	90.0	72.37(3)	96.430(10)
V/Å^3	4159.4(9)	13 798(6)	2058.1(7)
Z[a]	8	2	2
D_c/g cm^{-3}	1.370	1.586	1.579
μ/mm^{-1}	0.617	0.821	3.433
F(000)	1716	6534	974
Crystal size/mm	0.08 × 0.10 × 0.40	0.25 × 0.2 × 0.1	0.3 × 0.2 × 0.1
Crystal colour	Brown	Green	Green
θ range for data collection/°	3.41 to 25.86	1.95 to 26.00	2.76 to 74.80
Index ranges	$0 \le h \le 12$, $0 \le k \le 18$, $0 \le l \le 31$	$-22 \le h \le 22$, $-35 \le k \le 35$, $37 \le l \le 37$	$0 \le h \le 12$, $-16 \le k \le 16$, $-21 \le l \le 20$
No. of reflections collected	48 108	1009 003	8885
No. of unique reflections	3941	49 747	8378
R_{int}	0.068	0.094	0.043
Refinement method	Full-matrix LS on F^2	Full-matrix LS on F^2	Full-matrix LS on F^2
No. of parameters refined	268	3454	692
No. of applied constraints	45	497	59
wR_2[b] [for all F^2]	0.138	0.221	0.179
R_1 [for F with $F > 4\sigma(F)$]	0.052	0.072	0.063
No. of F with $F > 4\sigma(F)$	1745	14066	6037
S (Goodness-of-fit on F^2)	0.853	0.852	1.066
Final shift/esd, mean/max	0.000/0.000	0.000/0.001	0.000/0.000
Final $\Delta\rho_{max}$, $\Delta\rho_{min}$/*e* Å^{-3}	+0.38, −0.24	1.03, −0.49	+0.61, −0.54

[a] The formula unit, formula weight and multiplicity (*Z*) refer to the crystallographic asymmetric unit. [b] The weights of the F^2 values were calculated as $>\sigma^2(F^2) + (c_1P)^2 + c_2P]^{-1}$ where $P = (F_o^2 + 2F_c^2)/3$, and the constants c_1 and c_2 had the values 0.070 and 0.0 for **A**, 0.0868 and 0.0 for **C**, and 0.097 and 1.07 for **D**.

Published on 09 October 2006 on http://pubs.rsc.org | doi:10.1039/B604591J
Downloaded by University of California - Los Angeles on 01 January 2013

of the pyridyl ring planes in **C** also varies in a way that breaks up the crystallographic symmetry. As a consequence, each hexagon is without symmetry (*i.e.* asymmetric) in the latter case, although the pattern has crystallographic inversion symmetry, since four out of the eleven independent Cu^{2+} ions [Cu(8)–Cu(11), Fig. 3] are located on crystal inversion centres. On the other hand, the tri(pyridyl)triazine spacer moieties in the Cu-acetate complex[36] show identical flat conformations, thus leading to crystallographic symmetry for the created hexagonal rings in the complex framework. Yet, the endless two-dimensional polymeric layers pack in the very same way in both crystals, by being piled one upon the other, as shown in Fig. 4(b). Inspection of the inter-layer interactions and packing forces in the **C** crystals yielded a great number of shorter F···F, C···F and (C–)H···F approaches,[16,32,33] in agreement with the observations in the related **A** and **D** complexes (see below, and in Tables S1 and S4). However, the observed noteworthy symmetry-independent connections in **C** can hardly be listed in a Table of acceptable size.

(c) Coordination polymer D. In crystals, grown from chloroform solution, solvent molecules were also found to be included. The crystallographic asymmetric unit contains one chloroform together with one monomer unit (*i.e.* $CuC_{37}H_{17}F_{12}N_3O_4\cdot CHCl_3$), although there are two unique Cu centres [Cu(1) and Cu(2)] in the crystal, both located in special positions with site occupation factors (sof's) = 0.5 (Fig. 5). In spite of (C–)H···N hydrogen bond interaction from the chloroform guest to a pyridine nitrogen [N(3)] of the complex framework (Table S3†), the solvent molecule as well as the acceptor ring were found to exhibit static disorder. The observed disorder may be indicative of relatively weak interaction forces between the connected proton donor and acceptor groups in the (C–)H···N bonds. The mean values of five possible interactions (*cf.* Table S3; with the rms dispersion around the arithmetic average given in square brackets) are 3.2[1] Å for the C···N distances, 2.3[2] Å for the H···N contacts; and 153[10]° for the C–H···N angles [using calculated chloroform (C–)H disorder positions,[47] without correction or normalization].

The C(23)–C(27) pyridine ring (3) may occur in either of two partly overlapping disorder sites with the same probability [the refined group sof's are both 0.50(1)]. The unprimed and primed rings are planar to within 0.047 and 0.146 Å, respectively, and are tilted through 35.6(5)° with respect to each other. The included $CHCl_3$ molecule, on the other hand,

 This journal is © the Royal Society of Chemistry and the Centre National de la Recherche Scientifique 2006

View Article Online

Table 3 Selected geometric features[a] of the Cu^{2+} coordination polyhedra

Compound	Complex **A**	Complex **C**[b]	Complex **D**[c]	
Selected bond lengths/Å				
Cu–O (shorter)	1.996(3)	Vary from 1.983(6) to 2.091(8)	1.973(2)	1.989(2)
Cu–N	2.008(3)	Vary from 1.967(5) to 2.020(4)	1.999(3)	2.012(3)
Cu–O (longer)	2.266(3)	Vary from 2.157(8) to 2.305(7)	2.319(3)	2.303(2)
Cu–O (shorter) (mean)		2.04[3]	1.981[11]	
Cu–N (mean)		2.006[15]	2.006[9]	
Cu–O (longer) (mean)		2.25[4]	2.311[11]	
Selected bond angles/°				
N–Cu–N				
O (shorter)–Cu–O (shorter)	93.0(2)	Vary from 177.4(2) to 1797(2)	180.0	180.0
O (longer)–Cu–O (longer)	86.9(2)	Vary from 177.1(3) to 179.7(3)	180.0	180.0
N–Cu–N (mean)	173.3(2)	Vary from 175.5(3) to 179.8(3)	180.0	180.0
O (shorter)–Cu–O (shorter) (mean)		178.4[7]		
O (longer)–Cu–O (longer) (mean)		178.1[9]		
		177[2]		

[a] With esd's in parentheses for individual values; with the root mean square (rms) dispersion around the arithmetic average given in square brackets for the mean values; and without esd's for the values constrained by the crystal symmetry requirement. [b] Complex **C** contains eleven unique Cu-coordination polyhedra, of which four exhibit crystallographic inversion symmetry and seven do not. In the calculation of the mean values of the selected bond angles in the Table 3, the angles in only seven coordination polyhedra, which are not restricted by the crystallographic symmetry requirements, were taken into account. The corresponding angles in the remaining four polyhedra [around the Cu(8)–Cu(11) centres] are all 180°. [c] Complex **D** contains two unique Cu-coordination polyhedra, both with crystallographic inversion symmetry.

Published on 09 October 2006 on http://pubs.rsc.org | doi:10.1039/B604591J
Downloaded by University of California - Los Angeles on 01 January 2013

occupies at least three disorder sites, of which two partly overlap each other. The unprimed and primed chloroform sites have comparable occupancies [sof parameters are 0.43(7) and 0.41(6), respectively], whereas the third, double primed site seems to be populated with much lower probability [sof = 0.16(5)]. Worth noting is that in the final difference electron density ($\Delta\rho$) map some residual electron density ($\Delta\rho_{max}$ = 0.61 *e* $Å^{-3}$) was detected in the vicinity of the chloroform disorder sites, thus indicating the approximate character of the disorder model.

Both unique Cu^{2+} ions in **D** were found to occupy special positions, thus they are exactly at the centres of their respective coordination polyhedra due to the crystal symmetry requirement. In addition, the hfacac groups that coordinate to the same metal centre are also related by inversion symmetry. Hence, the two hfacac chelate ring planes joined to the same metal centre are co-planar in both cases. The chelate rings linked to Cu(1) were found to be approximately planar (both to within 0.102 Å), whereas the corresponding ones at Cu(2) are slightly puckered (envelope shaped, with the puckering parameters Q = 0.384 Å, θ = 123.1°, and φ = 168.9°).[27–29] The N–Cu–N(#) coordination angles in **D** are different from the corresponding one in **A**, but similar to those observed in crystal **C**, *i.e.* the polymer with the same tris(pyridylethynyl)-benzene bridging units between the metallic links [Table 3, Fig. 6(a)].

Although the tectonic ligand **3** is provided with three pyridyl N atoms in a trigonal arrangement, available for coordination to metal centres, one pyridyl nitrogen of each ligand molecule is engaged in a (C)–H···N hydrogen bond interaction[32] with the included chloroform solvent in crystal **D** (Fig. 5, Table S3). Consequently, the organic connecting link in **D** behaves only as bifunctional towards the metal ion, and the complex formation reaction leads to infinite one-dimensional polymeric chains [Fig. 6(a)], just as in complex **A**. The three pyridyl ring planes of the spacer moiety form distinctly different dihedral angles with the central benzene ring plane [78.1(1)°, 3.7(2) and 22.0(7), Table S2]. Worth noting is that, although each pyridine ring may have free rotation around the $C{\equiv}C{-}C_{py}\cdots N_{py}$ axis, the realized propeller-like conformation of ligand **3** in **D** resembles those observed for the related B, C, E and F spacer units in complex **C** (see above, and Table S2).

Inspection of the intermolecular or inter-chain contact distances in the solvated **D** complex yielded an impressive number of possible interactions [*e.g.* C–H···N, C–H···F, C–F···π, C–Cl···π, π···π][14,16,32,37,38] and various shorter connections (Table S4†), thus indicating denser packing in **D** than in **A**. A hypothetical packing coefficient, calculated by taking into account only the polymeric framework of **D** without the chloroform guest, is 60.0%.[29,30] Accordingly, the infinite ropes of complex **D** pack somewhat more efficiently than those of **A**.

The denser packing in **D** is probably a consequence of the more convenient shape of both the organic connecting link and the created polymeric chains, and also of the lower symmetry of crystal **D** (triclinic), as compared to that of **A** (orthorhombic). Moreover, chloroform molecules are included in the holes of the complex **D** framework [Fig. 6(b)] *via* $(C_{guest})H\cdots N_{py}$ hydrogen bonds[32] [$C_{guest}\cdots N_{py}$/$H_{guest}\cdots N_{py}$ distances are between 3.04(1)–3.35(3)/2.13–2.52 Å, C_{guest}–$H\cdots N_{py}$ angles range from 142 to 168°, Table S3]. In addition, the $CHCl_3$ molecules seem to be involved also in

Published on 09 October 2006 on http://pubs.rsc.org | doi:10.1039/B604591J
Downloaded by University of California - Los Angeles on 01 January 2013

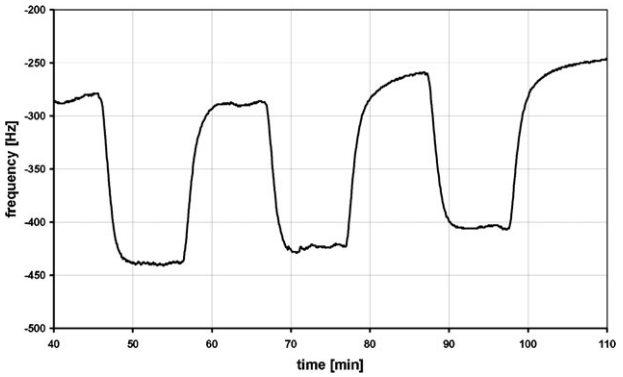

Fig. 7 Sensor reaction of a polymer **A**-coated QMB sensor in three cycles of adsorption and desorption, each during an exposure to methanol.

(C)–Cl$\cdots\pi_{ethynyl}$ interactions[15a] with the host framework [Cl$\cdots\pi_{ethynyl}$ distances are between 3.219(6)–3.561(8) Å, C–Cl$\cdots\pi_{ethynyl}$ angles range from 147(2) to 152.6(7)°, Table S3]. In spite of these host–guest interactions, the included solvent molecule was found to exhibit static disorder by occurring at least at three different disorder sites (Fig. 5). Worth mentioning is that the chloroform molecule seems to be engaged in almost the same interaction modes with the surrounding complex framework in all of its three disorder sites. At the same time, the available space within each void is obviously big enough to allow static disorder for a molecule of chloroform size. According to the calculations,[29] the solvent molecules reside in voids of about 165 Å^3 each, and occupy a total of 330 Å^3 (~16%) of the unit cell volume, thus further enhancing the crystal packing density. The estimated crystal packing index[29,30] is as high as 72.2%, and there is no residual solvent accessible volume to be found in the solvated **D** crystal.

Sensor behaviour on a quartz micro balance (QMB)

In a first screening, the porous polymeric compound **A** was studied with respect to the sensor reaction for potential analysis of volatile compounds such as alcohols (methanol, ethanol, *n*-propanol, isopropanol, *n*-butanol), ketones (acetone, butanone), esters (ethyl acetate, ethyl formate), hydrocarbons (*n*-hexane, toluene, limonene) and water, respectively. The screening shows interesting reactions of this coordination polymer, indicating a reversible response of relatively small and polar analytes. They include methanol (Fig. 7), ethanol and acetone, but not water. These successful analyte molecules are small enough for free mobility in the channels of the network. The quality of the pore walls (hydrophobic and hydrophilic sites) may explain the reaction of the mentioned analytes.[38] The results support potential application of the coordination polymer as coating material in QMB sensors.[39]

Conclusion

In this paper we have described the synthesis, the spectroscopic characterization and the crystal structures of novel coordination polymers based on pyridine-containing linear or trigonal tectonic ligands and copper(II) hexafluoroacetylacetonate. The complex compounds proved to form polymeric ropes (**A** and **D**) or sheets (**C**). The structural characteristics of the tectonic spacer units, and the number of their functional groups, available for coordination to metal ions, are crucial for the geometry of the polymeric frameworks. In one case (**D**) organic solvent molecules of chloroform were found to be included and to obstruct one of the coordination sites of the trivalent tecton, thus giving rise to a cross between one-dimensional coordination polymer and crystalline solvent inclusion. The porous polymeric crystals, held together by relatively weak interaction forces, proved to have a potential for inclusion formation and/or sensor behaviour.[2b,3b] The results of the screening of volatile compounds confirm potential application of the coordination polymers as coating material in QMB sensors.[39]

Thus, using a combination of geometrically defined pyridine-containing spacer-type organic ligands and coordinatively unsaturated Cu(II) hexafluoroacetylacetonate moieties, with the fluoro substitution being determinant, yielded a successful approach to the formation of new, porous metal–organic hybrid structures. Future modifications of the organic spacer unit from two- to three-dimensional construction are expected to open a range of promising coordination lattices.

Experimental

Equipment

Melting points were determined with a microscope hot plate (Dresden Analytik). IR spectra were recorded with a Nicolet FT-IR spectrometer 510 in the 400–4000 cm^{-1} spectral range. ^{1}H and ^{13}C NMR spectra were obtained with a Bruker DPX 400 spectrometer with $(CH_3)_4Si$ as internal standard. Mass spectra were recorded with HP 59987A (ESI) and HP 5890 series II/MS (5989A and 5971, GC-MS) instruments. Elemental analyses were performed with a Heraeus CHN-O Rapid elemental analyser.

Materials

The solvents were of analytical grade and were used without further purification. Reagents and materials were obtained from commercial suppliers (Aldrich, Avocado, Fluka) and were used without further purification. The coupling reactions were carried out under argon and monitored by TLC (Merck, silica gel 60 F_{254}-coated plates). For column chromatography, neutral alumina was used (Fluka, Brockmann activity I, pH 7.0 ± 0.5, particle size 0.05–0.15 mm).

Synthesis

9,10-Dibromoanthracene, 1,5-dibromoanthracene and 1,3,5-tribromobenzene. These were prepared by bromination of anthracene,[40] substitution of bromine for chlorine in 1,5-dichloroanthraquinone, followed by reduction to the 1,5-substituted anthracene,[41] and deamination of 2,4,6-tribromoaniline,[42] respectively, according to the literature procedures.

4-Ethynylpyridine. This was obtained by a palladium-assisted coupling reaction of 4-bromopyridine hydrochloride with 2-methyl-3-butyn-2-ol (MEBYNOL),[22] followed by alkaline hydrolysis of the protecting group in 85%, according to the literature description.[22]

 This journal is © the Royal Society of Chemistry and the Centre National de la Recherche Scientifique 2006

Published on 09 October 2006 on http://pubs.rsc.org | doi:10.1039/B604591J
Downloaded by University of California - Los Angeles on 01 January 2013

9,10-Bis[2-(4-pyridyl)ethynyl]anthracene (1)[20]. A mixture of 9,10-dibromoanthracene (0.89 g, 2.6 mmol) and 4-ethynylpyridine (0.6 g, 5.8 mmol) was dissolved in boiling triethylamine–toluene (1 : 1, v/v, 50 ml). A stream of argon was bubbled through the boiling solution for about 30 min in order to free it from air. After cooling to room temperature, a catalyst mixture composed of palladium(II) acetate (12.5 mg), triphenylphosphane (37.5 mg) and copper(I) iodide (12.5 mg) was added, and the solution was heated under reflux for 1 d. The solvent was removed under reduced pressure, and the residue was stirred with water for 2 h to extract the triethylammonium salt. The solid was filtered and dried *in vacuo*. Recrystallization from toluene yielded 61% (0.6 g) orange needles: mp 302–308 °C. Anal. calcd $C_{28}H_{16}N_2$ (380.4) · H_2O: C 84.40, H 4.55, N 7.03; found C 84.12, H 4.33, N 7.15%. IR (KBr): $\tilde{\nu}$ = 3070–3026 (arom. CH), 2208 (C≡C), 1618, 1589–1405 (Ar), 828 (4-monosubst. pyridine), 811, 770 cm^{-1}. ^1H NMR (400.1 MHz, $CDCl_3$): δ = 7.6 (m, 4 H, PyH), 7.7 (dd, ^3J(H,H) = 6.7 Hz, ^4J(H,H) = 3.1 Hz, 4 H, ArH), 8.7 ppm (dd, 4 H, PyH). ^{13}C NMR (100.6 MHz, $CDCl_3$): δ = 90.6, 99.1 (C≡C), 118.2, 125.5, 127.0, 127.5, 131.2, 132.3, 150.1 ppm; MS (+ESI): m/z (%) = 381 (100) [M^+], 191 (57) [M^{2+}].

1,5-Bis[2-(4-pyridyl)ethynyl]anthracene (2). A mixture of 1,5-dibromoanthracene (2.18 g, 6.5 mmol) and 4-ethynylpyridine (1.5 g, 14.5 mmol) was dissolved in boiling triethylamine–toluene (1 : 1, v/v, 50 ml). Addition of catalyst [Pd(II) acetate: 31.3 mg, PPh_3: 108.8 mg and Cu(I)I: 31.3 mg], reaction conditions and workup as above, except for the purification of the product, which was performed by column chromatography (silica gel, ethyl acetate), yielded 45% (1.11 g) of a brown-orange solid: mp >360 °C. Anal. calcd for $C_{28}H_{16}N_2$ (380.4) · 0.5 H_2O: C 86.35, H 4.40, N 7.19; found C 86.52, H 4.39, N 6.98%. IR (KBr): $\tilde{\nu}$ = 3068–3020 (arom. CH), 2209 (C≡C), 1605, 1592–1415 (Ar), 879 (9,10-positions of anthracene), 819 (4-monosubst. pyridine), 726 cm^{-1}. ^1H NMR (400.1 MHz, $CDCl_3$): δ = 7.6 (m, 6 H, ArH, PyH), 7.9 (d, ^3J(H,H) = 6.7 Hz, 2 H, ArH), 8.2 (d, 2 H, ^3J(H,H) = 8.2 Hz, ArH), 8.7 (d, 4 H, ^3J(H,H) = 5.1 Hz, PyH), 9 ppm (s, 2 H, ArH). ^{13}C NMR (100.6 MHz, $CDCl_3$): δ = 92.1, 92.1 (C≡C), 119.9, 125.3, 125.6, 125.7, 130.5, 131.1, 131.4, 131. 7, 131.8, 150.0 ppm. MS (+ESI): m/z (%) = 381 (100) [M^+].

1,3,5-Tris[2-(4-pyridyl)ethynyl]benzene (3). A mixture of 1,3,5-tribromobenzene (1.03 g, 3.27 mmol) and 4-ethynylpyridine (1.3 g, 12.6 mmol) was dissolved in boiling triethylamine (90 ml). A stream of argon was bubbled through the boiling solution for about 30 min in order to free it from air. After cooling to room temperature, a catalyst of tetrakis(triphenylphosphine)palladium(0) (244 mg) was added, and the mixture was refluxed for 3 d. The solvent was removed under reduced pressure, and the residue was dissolved in dichloromethane. The solution was washed with water (3 × 150 ml), dried (Na_2SO_4), and concentrated. Column chromatography (neutral Al_2O_3, dichloromethane–ethanol 1–2%) yielded 53% (0.66 g) of white needles: mp 237 °C (decomp.). Anal. calcd for $C_{27}H_{15}N_3$ (381.3): C 85.02, H 3.96, N 11.02; found C 84.74, H 4.09, N 10.83%. IR (KBr): $\tilde{\nu}$ = 3076 (arom. CH), 2217 (C≡C), 1597, 1539, 1491, 1408 (Ar), 882 (1,3,5-trisubst. benzene), 820 cm^{-1} (4-monosubst. pyridine). ^1H NMR (400.1 MHz, $CDCl_3$): δ = 7.4 (m, 6 H, PyH), 7.8 (s, 3 H, ArH), 8.6 ppm (m, 6 H, PyH). ^{13}C NMR (100.6 MHz, $CDCl_3$): δ = 88.3, 91.4 (C≡C), 123.4, 125.5, 130.6, 135.2, 149.9 ppm. MS (GC-MS): m/z (%) = 381 (100) [M^+], 190 (8) [M^{2+}].

General procedure for the synthesis of coordination polymers. Separate chloroform solutions containing stoichiometric amounts of ligand (**1**, **2** or **3**) and copper(II) hexafluoroacetylacetonate were prepared. The salt solution was slowly added dropwise to the ligand solution, and the mixture was stirred for 3 h at room temperature. The precipitate was collected by filtration, washed with chloroform and dried.

Bis(1,1,1,5,5,5-hexafluoro-2,4-pentanedionato)-*cis*-μ-{9,10-bis[2-(4-pyridyl)ethynyl]-anthracene-*N*:*N*′}copper(II) 1D coordination polymer (A). 89% yield of a red-brown microcrystalline solid: mp 272 °C (dec.). Anal. calcd for $C_{38}H_{18}CuF_{12}N_2O_4$ (858.1): C 53.19, H 2.11, N 3.26; found C 53.12, H 2.19, N 3.38%. IR (KBr): $\tilde{\nu}$ = 2197 (C≡C), 1671 (C═O), 1646–1599 (C═C, C═O, Ar), 1532–1512 (CH chelate ring), 1256 (C═C chelate ring), 1203, 1151 (CF_3), 823 (4-monosubst. pyridine), 791 (CF_3), 662 (chelate ring), 577 cm^{-1} (CF_3, Ar).

Bis(1,1,1,5,5,5-hexafluoro-2,4-pentanedionato)-*cis*-μ-{1,5-bis[2-(4-pyridyl)ethynyl]-anthracene-*N*:*N*′}copper(II) 1D coordination polymer (B). 70% yield of a lemon-yellow–green microcrystalline solid: mp 288 °C (decomp.). Anal. calcd for $C_{38}H_{18}CuF_{12}N_2O_4$ (858.1): C 53.19, H 2.11, N 3.26; found C 52.94, H 2.25 N 3.33%. IR (KBr): $\tilde{\nu}$ = 2208 (C≡C), 1669 (C═O), 1646–1613 (C═C, C═O, Ar), 1532–1509 (CH chelate ring), 1257 (C═C chelate ring), 1210, 1150 (CF_3), 879 (9,10-positions of anthracene), 831 (4-monosubst. pyridine), 794 (CF_3), 662 (chelate ring), 577 cm^{-1} (CF_3, Ar).

***trans*-Hexakis(1,1,1,5,5,5-hexafluoro-2,4-pentanedionato)-bis{-μ$_3$-(1,3,5-tris[2-(4-pyridyl)ethynyl]benzene-*N*:*N*′:*N*″)}tricopper(II) 2D coordination polymer (C).** 66% yield of a light green powder: mp 270 °C (decomp.). Anal. calcd for $C_{42}H_{18}Cu_{1.5}F_{18}N_3O_6$ (1097.9): C 45.95, H 1.65, N 3.83; found C 46.07, H 1.74, N 3.84%. IR (KBr): $\tilde{\nu}$ = 2218 (C≡C), 1671 (C═O), 1647-1601 (C═C, C═O, Ar), 1532–1513 (CH chelate ring), 1257 (C═C chelate ring), 1203, 1148 (CF_3), 883 (1,3,5-trisubst. benzene), 829 (4-monosubst. pyridine), 792 (CF_3), 662 (chelate ring), 578 cm^{-1} (CF_3).

X-Ray crystallographic study

Single-crystals of the coordination polymers **A** and **C**, suitable for diffraction studies, were obtained by slow diffusion at room temperature between a chloroform–benzene or chloroform solution of **1** or **3**, respectively, and a superposed layer of an ethanol solution of copper(II) hexafluoroacetylacetonate. The same approach was used also for obtaining crystals of the chloroform-solvated coordination polymer **D**, containing ligand **3** and Cu(hfacac)$_2$ in the ratio 1 : 1.

X-Ray intensity data for complexes **A** and **C** were collected on a STOE IPDS (Imaging Plate Detection System)[43] instrument equipped with a rotating anode (MoKα radiation), whereas a CAD-4 (Enraf Nonius) diffractometer[44] and a

View Article Online

Downloaded by University of California - Los Angeles on 01 January 2013
Published on 09 October 2006 on http://pubs.rsc.org | doi:10.1039/B604591J

conventional X-ray tube (CuKα radiation) were used for coordination polymer **D**. The net intensities were corrected for Lorentz, polarization[43,45] and absorption effects. Numerical absorption corrections[46] were applied for complexes **A** and **C** (transmission varied between 0.78 and 0.91, and 0.82 and 0.90, respectively). The crystals of the chloroform-containing **D** polymer, however, were extremely unstable. Due to practical problems in connection to the data collection, and for lack of a second single crystal of acceptable quality, the collected data had to be corrected by empirical methods (the virtual transmission varied between 0.28 and 0.73).

Programs of the SHELX-97[47] system were used for the solution and refinement calculations of complexes **A** and **D**, whereas the size of the problem connected with the structure of complex **C** required special versions of the SHELXS[47] and SHELXL[47] programs (see below). The non-hydrogen positions and possible disorder sites (*e.g.* in **D**) were refined together with their anisotropic displacement parameters in all cases. The partially occupied non-hydrogen positions in **D** had to be refined with simple distance constraints in order to get acceptable geometry for the disorder models (Table 2). The hydrogen atoms were placed at positions calculated using geometric evidence,[47] and isotropic displacement parameters were refined for them. The LS calculation indicated relatively large mobility or disorder for the CF_3 groups of the Cu(hfcaca)$_2$ entities, particularly in complexes **A** and **C** with X-ray data collected at room temperature. Accordingly, the calculated mean values for the U_{eq} (F) parameters are 0.24[9] in **A**, 0.22[6] in **C**, but only 0.11[3] Å^2 in **D** (with the rms deviation given in square brackets). Since the assumed disorder of the CF_3 groups could not be resolved into distinct disorder sites in the present cases, soft distance constraints had to be applied in the refinement of these groups in **A** and **C** (see below) (Table 2).

Crystals of the coordination polymer **C** (Scheme 4) proved to have a remarkably large unit cell of 13 795(6) Å^3, containing as much as 846 non-hydrogen atoms (Table 2), and exhibiting relatively low symmetry (triclinic $P\bar{1}$). The unique fragment of the infinite two-dimensional framework consists of altogether nine Cu(hfcaca)$_2$ entities, linked together by six tris(pyridylethynyl)benzene units (A–F) (Fig. 5). Seven copper centres [Cu(1)–Cu(7)] occupy general positions, whereas an additional four [Cu(8)–Cu(11)] are located at special positions (each with 50% site occupation). Accordingly, in the course of the X-ray structure analysis, 423 non-hydrogen atoms (9 Cu, 252 C, 36 O, 18 N and 108 F) had to be located and refined, thus creating a problem of unusual size and complexity. The phase problem was solved using the program SHELXD,[48] and refinement of the 3454 parameters against 49 747 F_{obs}^2 values required SHELXH, the large-memory version of the SHELXL-97 program.[47] Moreover, the calculations indicated relatively high mobility or disorder for a number of fluoro substituents [U_{eq} (max) = 0.38(1) Å^2 for F(58)], and also for a few carbon atoms [U_{eq} (max) = 0.22(1) Å^2 for C(3F1)]. In the final least-squares calculation, the CF_3 groups were refined with soft distance constraints, whereas the six-membered aromatic rings were held riding on their C(1)/N(1) atoms, respectively, in order to maintain acceptable geometry for them. The (C)–H atoms were included at idealized positions.[47] Both the highest electron density peak ($\Delta\rho_{max}$ = 1.03 *e* Å^{-3}) and the deepest hole ($\Delta\rho_{min}$ = −0.49 *e* Å^{-3}) in the final $\Delta\rho$ map were found to be located in the vicinity of a heavy atom [0.99 and 0.88 Å from Cu(4), respectively].

Crystal data together with further details of data collection, data reduction and refinement calculations are presented in Table 2.‡

Sensorial screening experiments

The quartz microbalance (QMB) sensors employed were commercially available 10 MHz AT-cut quartz crystals (1.37 cm diameter) with gold electrodes (0.51 cm diameter) on both sides, purchased from FOQ, Bad Rappenau, Germany. The frequency of the vibrating crystal was measured with a universal frequency counter connected to a personal computer. The frequency data were recorded every 10 s.

The coating material composed of **A** was prepared by drop coating of a fine suspension of the coordination polymer in acetone (generated with ultrasound) with a µl-syringe onto the centre of the electrode of the crystal. The solvent was evaporated in air, and the quartz crystal was stored in a desiccator for 10 h.

The screening experiments with the coated quartz crystals were carried out in a flow chamber at room temperature. In order to adjust the baseline, the chamber was flushed with dry air. Then, a stream of air saturated with the analyte solvent was passed into the chamber. After 20 min duration of action, the frequency shift was determined. For regeneration, the quartz crystals were purged with dry air for 20 min, and reused. For each solvent, the process was repeated three times (Fig. 8). The measured values were adjusted to a standard thickness of the sensor film corresponding to 10 kHz frequency shift, allowing reasonable comparison of the data.[49]

Acknowledgements

This work was supported by the German Ministry of Education and Research (BMBF-Project "Biomon" 02110120) and the Fonds der Chemischen Industrie.

References

1 (*a*) *Comprehensive Supramolecular Chemistry*, ed. G. Alberti and T. Bein, Elsevier, Oxford, 1996, vol. 7; (*b*) C. J. Jones, *Chem. Soc. Rev.*, 1998, **27**, 289–300; (*c*) R. W. Saalfrank and B. Demleitner, in *Transition Metals in Supramolecular Chemistry*, ed. J. P. Sauvage, Wiley-VCH, Weinheim, 1999, pp. 1–51; (*d*) P. J. Hagrman, D. Hagrman and J. Zubieta, *Angew. Chem.*, 1999, **111**, 2798–2848; (*e*) L. F. Lindoy, *Angew. Chem., Int. Ed.*, 1999, **38**, 2638–2684; (*f*) L. F. Lindoy and I. M. Atkinson, *Monographs in Supramolecular Chemistry*, Royal Society of Chemistry, Cambridge, UK, 2000, vol. 7; (*g*) G. Swiegers and T. J. Malefetse, *Chem. Rev.*, 2000, **100**, 3483–3537; (*h*) M. D. Ward, J. A. McCleverty and J. C. Jeffery, *Coord. Chem. Rev.*, 2001, **222**, 251–272; (*i*) C. N. R. Rao, S. Natarajan and R. Vaidhyanathan, *Angew. Chem.*, 2004, **116**, 1490–1521; (*j*) M. Ruben, *Angew. Chem., Int. Ed.*, 2004, **43**, 1466–1496; (*k*) M. Ruben, J. Rojo, F. J. Romero-Salguero, L. H. Uppadine and J.-M. Lehn, *Angew. Chem.*, 2004, **116**, 3728–3747; (*l*) M. Ruben, J. Rojo, F. J. Romero-Salguero, L. H. Uppadine and J.-M. Lehn, *Angew. Chem., Int. Ed.*, 2004, **43**, 3644–3662.

‡ CCDC reference numbers 290977–290979. For crystallographic data in CIF or other electronic format see DOI: 10.1039/b604591j

 This journal is © the Royal Society of Chemistry and the Centre National de la Recherche Scientifique 2006

View Article Online

Downloaded by University of California - Los Angeles on 01 January 2013
Published on 09 October 2006 on http://pubs.rsc.org | doi:10.1039/B604591J

2 (*a*) J. A. McCleverty, T. J. Meyer, M. Fujita, A. Powell and C. A. Creutz, *Comprehensive Coordination Chemistry*, Elsevier, Oxford, 2004, vol. 7; (*b*) T. Hertzsch, J. Hulliger, E. Weber and P. Sozzani, in *Encyclopedia of Supramolecular Chemistry*, ed. J. Atwood and J. Steed, Marcel Dekker, New York, 2004, pp. 996–1005.
3 (*a*) P. R. Andres and U. Schubert, *Adv. Mater*., 2004, **16**, 1043–1068; (*b*) S. Kitagawa, R. Kitaura and S. Noro, *Angew. Chem*., 2004, **116**, 2388–2430; (*c*) S. Kitagawa, R. Kitaura and S. Noro, *Angew. Chem., Int. Ed*., 2004, **43**, 2334–2375; (*d*) J. L. C. Rowsell and O. M. Yaghi, *Angew. Chem*., 2005, **117**, 4748–4758; (*e*) J. L. C. Rowsell and O. M. Yaghi, *Angew. Chem., Int. Ed*., 2005, **44**, 4670–4679.
4 K. Biradha and M. Fujita, *J. Incl. Phenom*., 2001, **49**, 201–208.
5 (*a*) M. A. Withersby, A. J. Blake, N. R. Champness, P. Hubberstey, W.-S. Li and M. Schröder, *Angew. Chem*., 1997, **109**, 2421–2423; (*b*) M. A. Withersby, A. J. Blake, N. R. Champness, P. Hubberstey, W.-S. Li and M. Schröder, *Angew. Chem., Int. Ed. Engl*., 1997, **36**, 2327–2329; (*c*) K. A. Hirsch, S. R. Wilson and J. F. Moore, *Inorg. Chem*., 1997, **36**, 2960–2969.
6 (*a*) M. A. Withersby, A. J. Blake, N. R. Champness, P. A. Cooke, P. Hubberstey, W.-S. Li and M. Schröder, *Inorg. Chem*., 1999, **38**, 2259–2266; (*b*) S. Lee, D. M. Shin and Y. K. Chung, *Chem.–Eur. J*., 2004, **10**, 3158–3165.
7 B. Moulton and M. J. Zaworotko, *Chem. Rev*., 2001, **101**, 1629–1658.
8 (*a*) K. Biradha, Y. Hongo and M. Fujita, *Angew. Chem*., 2000, **112**, 4001–4003; (*b*) K. Biradha, Y. Hongo and M. Fujita, *Angew. Chem., Int. Ed*., 2000, **39**, 3843–3845; (*c*) N. G. Pschirer, D. M. Ciurtin, M. D. Smith, U. H. F. Bunz and H.-G. zur Loye, *Angew. Chem*., 2002, **114**, 603–605; (*d*) G. Pschirer, *Angew. Chem., Int. Ed*., 2002, **41**, 583–585; (*e*) Z. Xu, Y.-H. Kiang, S. Lee, E. B. Lobkovsky and N. Emmott, *J. Am. Chem. Soc*., 2000, **122**, 8376–8391; (*f*) G. K. Patra and I. Goldberg, *J. Chem. Soc., Dalton Trans*., 2002, 1051–1057.
9 (*a*) S. R. Batten and R. Robson, *Angew. Chem*., 1998, **110**, 1558–1595; (*b*) S. R. Batten and R. Robson, *Angew. Chem., Int. Ed*., 1998, **37**, 1460–1494.
10 (*a*) B. F. Abrahams, S. R. Batten, H. Hamit, B. F. Hoskins and R. Robson, *Chem. Commun*., 1996, 1313–1314; (*b*) S. L. James, *Chem. Soc. Rev*., 2003, **32**, 276–288; (*c*) D. N. Dybtsev, H. Chun and K. Kim, *Angew. Chem*., 2004, **116**, 5143–5146; (*d*) D. N. Dybtsev, H. Chun and K. Kim, *Angew. Chem., Int. Ed*., 2004, **43**, 5033–5036.
11 (*a*) G. R. Desiraju, *Crystal Engineering, The Design of Organic Solids*, Elsevier, Amsterdam, 1989; (*b*) G. R. Desiraju, *Angew. Chem*., 1995, **107**, 2541–2558; (*c*) G. R. Desiraju, *Angew. Chem., Int. Ed. Engl*., 1995, **34**, 2311–2327; (*d*) *Design of Organic Solids, Topics in Current Chemistry*, ed. E. Weber, Springer-Verlag, Berlin-Heidelberg, 1998, vol. 198; (*e*) *Crystal Design – Structure and Function, Perspectives in Supramolecular Chemistry*, ed. G. R. Desiraju, Wiley, Chichester, 2003, vol. 7.
12 *Molecular Self-Assembly—Organic Versus Inorganic Approaches, Structure and Bonding*, ed. M. Fujita, Springer-Verlag, Berlin–Heidelberg, 2000, vol. 96.
13 D. Braga, L. Brammer and N. R. Champness, *CrystEngComm*, 2005, **7**, 1–19.
14 (*a*) J. D. Dunitz and A. Gavezzotti, *Angew. Chem*., 2005, **117**, 1796–1819; (*b*) J. D. Dunitz and A. Gavezzotti, *Angew. Chem., Int. Ed*., 2005, **44**, 1766–1787.
15 (*a*) J. D. Dunitz and R. Taylor, *Chem.–Eur. J*., 1997, **3**, 89–98; (*b*) M. D. Prasanna, T. N. Guru and Row, *Cryst. Eng*., 2000, **3**, 135–154; (*c*) G. R. Desiraju and R. Partasarathy, *J. Am. Chem. Soc*., 1989, **111**, 8725–8726; (*d*) V. R. Thalladi, H.-C. Weiss, D. Bläser, R. Boese, A. Nangia and G. R. Desiraju, *J. Am. Chem. Soc*., 1998, **120**, 8702–8710; (*e*) A. R. Choudhury and T. N. Guru Row, *Cryst. Growth Des*., 2004, **4**, 47–52.
16 K. Reichenbächer, H. I. Süss and J. Hulliger, *Chem. Soc. Rev*., 2005, **34**, 22–30.
17 (*a*) M. Fujita, S. Nagao, M. Iida, K. Ogata and K. Ogura, *J. Am. Chem. Soc*., 1993, **115**, 1574–1576; (*b*) K. Kasai, M. Aoyagi and M. Fujita, *J. Am. Chem. Soc*., 2000, **122**, 2140–2141; (*c*) K. Reichenbächer, H. I. Süss, H. Stoeckli-Evans, S. Bracco, P. Sozzani, E. Weber and J. Hulliger, *New J. Chem*., 2004, **28**, 393–397.
18 (*a*) B. J. Holliday and C. A. Mirkin, *Angew. Chem*., 2001, **113**, 2076–2098; (*b*) B. J. Holliday and C. A. Mirkin, *Angew. Chem., Int. Ed*., 2001, **40**, 2022–2043.
19 (*a*) K. Sonogashira, Y. Tohda and N. Hagihara, *Tetrahedron Lett*., 1975, **16**, 4467–4470; (*b*) S. Takahashi, Y. Kuroyama, K. Sonogashira and N. Hagihara, *Synthesis*, 1980, 627–630.
20 T. M. Fasina, J. C. Collings, D. P. Lydon, D. Albesa-Jove, A. S. Batsanov, J. A. K. Howard, P. Nguyen, M. Bruce, A. J. Scott, W. Clegg, S. W. Watt, C. Viney and T. B. Marder, *J. Mater. Chem*., 2004, **14**, 2395–2404.
21 (*a*) H. L. Anderson, C. J. Walter, A. Vidal-Ferran, R. A. Hay, P. A. Lowden and J. K. M. Sanders, *J. Chem. Soc., Perkin Trans. 1*, 1995, 2275–2279; (*b*) P. J. Stang, B. Olenyuk, D. C. Muddiman and R. D. Smith, *Organometallics*, 1997, **16**, 3094–3096.
22 (*a*) L. D. Ciana and A. Haim, *J. Heterocycl. Chem*., 1984, **21**, 607–608; (*b*) J. G. Rodriguez, R. Martin-Villamil, F. H. Cano and I. Fonseca, *J. Chem. Soc., Perkin Trans. 1*, 1997, 709–714.
23 S. Leininger, B. Olenyuk and P. J. Stang, *Chem. Rev*., 2000, **100**, 853–908.
24 (*a*) C. J. Kuehl, T. Yamamoto, S. R. Seidel and P. J. Stang, *Org. Lett*., 2002, **4**, 913–915; (*b*) S.-S. Sun, J. A. Anspach and A. J. Lees, *Inorg. Chim. Acta*, 2003, **351**, 363–368; (*c*) M. Schweiger, T. Yamamoto, P. J. Stang, D. Bläser and R. Boese, *J. Org. Chem*., 2005, **70**, 4861–4864; (*d*) D. C. Caskey and J. Michl, *J. Org. Chem*., 2005, **70**, 5442–5448.
25 (*a*) D. Gibson, B. F. G. Johnson and J. Lewis, *J. Chem. Soc. A*, 1970, **1**, 367–369; (*b*) L. Zanotto, F. Benetollo, M. Natali, G. Rosetto, P. Zanella, S. Kaciulis and A. Mezzi, *Chem. Vap. Deposition*, 2004, **10**, 207–213.
26 S. Winter, W. Seichter and E. Weber, *Z. Anorg. Allg. Chem*., 2004, **630**, 434–442.
27 D. Cremer and J. A. Pople, *J. Am. Chem. Soc*., 1975, **97**, 1354–1367.
28 J. A. Boeyens, *J. Cryst. Mol. Struct*., 1978, **8**, 317–320.
29 A. L. Spek, *PLATON, A Multi Purpose Crystallographic Tool (Version 111 203)*, 1980–2003.
30 A. I. Kitaigorodsky, *Molecular Crystals and Molecules*, Academic Press, New York, 1973.
31 A. Bondi, *J. Phys. Chem*., 1964, **68**, 441–451.
32 G. R. Desiraju and T. Steiner, *The Weak Hydrogen Bond* (IUCr Monographs on Crystallography, vol. 9), Oxford University Press, New York, 1999, pp. 202–209.
33 M. Nishio, in *Encyclopedia of Supramolecular Chemistry*, ed. J. L. Atwood, J. W. Steed, Marcel Dekker, New York, 2004, pp. 1576–1585.
34 A. Schwarzer, W. Seichter, E. Weber, H. Stoeckli-Evans, M. Losada and J. Hulliger, *CrystEngComm*, 2004, **6**, 567–572.
35 I. Csöregh, M. Czugler and E. Weber, *J. Phys. Org. Chem*., 1993, **6**, 171–178.
36 S. R. Batten, B. F. Hoskins, B. Moubaraki, K. S. Murray and R. Robson, *Chem. Commun*., 2000, 1095–1096.
37 C. A. Hunter and J. K. M. Sanders, *J. Am. Chem. Soc*., 1990, **112**, 5525–5534.
38 E. Choi, K. Park, C. Yang, H. Kim, J. Son, S. W. Lee, Y. H. Lee, D. Min and Y. Kwon, *Chem.–Eur. J*., 2004, **10**, 5535–5540.
39 (*a*) F. L. Dickert, H. Stathopulos and M. Reif, *Adv. Mater*., 1996, **8**, 525–529; (*b*) K. Matsuura, K. Ariga, K. Endo, Y. Aoyama and Y. Okahata, *Chem.–Eur. J*., 2000, **6**, 1750–1756.
40 H. Gilman and A. H. Blatt, *Organic Synthesis*, Wiley, New York, 1941, vol. 1, pp. 207–208.
41 M. J. Brienne and J. Jaques, *Bull. Soc. Chim. Fr*., 1973, 190–197.
42 Jackson and Bentley, *Am. Chem. J*., 1892, **14**, 335–336.
43 STOE & CIE GmbH, 1997 (publications 4805-014).
44 CAD-4 software, Version 5; Enraf Nonius, Delft, The Netherlands.
45 A. L. Spek, *HELENA, Program for Data Reduction*, Utrecht University, The Netherlands, 2003.
46 STOE & CIE GmbH, X-shape and X-red programs, 1997.
47 G. M. Sheldrick, *SHELXS–97 and SHELXL–97*, University of Göttingen, Germany, 1997.
48 G. M. Sheldrick, *SHELXD*, University of Göttingen, Germany, 2002.
49 (*a*) U. Schramm, C. E. O. Roesky, S. Winter, T. Rechenbach, P. Boeker, P. Schulze Lammers, E. Weber and J. Bargon, *Sens. Actuators, B*, 1999, **57**, 233–237; (*b*) T. Rechenbach, U. Schramm, P. Boeker, G. Horner, C. E. O. Roesky, J. Trepte, S. Winter, R. Pollex, J. Bargon, E. Weber and P. Schulze Lammers, *Sens. Actuators, B*, 1999, **57**, 255–260.